Hippocampal awake replay in fear memory retrieval

Chun-Ting Wu[1,2], Daniel Haggerty[2], Caleb Kemere[3] & Daoyun Ji[2,4]

Hippocampal place cells are key to episodic memories. How these cells participate in memory retrieval remains unclear. After rats acquired a fear memory by receiving mild footshocks in a shock zone on a track, we analyzed place cells when the animals were placed on the track again and displayed an apparent memory retrieval behavior: avoidance of the shock zone. We found that place cells representing the shock zone were reactivated, despite the fact that the animals did not enter the shock zone. This reactivation occurred in ripple-associated awake replay of place cell sequences encoding the paths from the animal's current positions to the shock zone but not in place cell sequences within individual cycles of theta oscillation. The result reveals a specific place-cell pattern underlying inhibitory avoidance behavior and provides strong evidence for the involvement of awake replay in fear memory retrieval.

The hippocampus is critical for episodic memory[1,2]. A cardinal feature of episodic memory is its link to particular spatial environments or contexts where events take place[3]. It is proposed that spatial environments of episodic memory are encoded by hippocampal place cells[4–6], which fire at specific spatial locations (place fields)[7,8]. For example, in contextual fear conditioning, after receiving mild footshocks in a box, animals subsequently display fear responses, such as freezing inside the box or avoiding entering the box[9], which indicate that the animals associate the aversive shock experience with this particular environment. Notably, these fear responses are hippocampus-dependent[10,11], presumably due to the critical role hippocampal place cells play in encoding spatial contexts of the box. Consistent with this idea, optogenetic manipulation of those hippocampal cells active in the box leads to impaired or false fear memory responses[12–14]. However, direct neurophysiological evidence for place cells encoding spatial environments of fear memory has been lacking.

We set out to provide such neurophysiological evidence. We reasoned that, if place cells encode environments of aversive experience, the same neurons should be reactivated during later contextual fear memory retrieval, even if retrieval occurs in places not directly associated with aversion. Reactivation of specific place cells has been demonstrated during awake behavior. For example, when rats travel through a linear track, place cells in the hippocampal CA1 area fire one after another in a sequence. During eating or when pausing or stopping on the track, the same firing sequence is reactivated within brief periods of 50–400 ms, which are characterized by high-frequency (100–250 Hz) ripple oscillations in the local field potentials (LFPs)[15–22]. It is proposed that this 'awake replay' serves as a neural substrate of memory retrieval[23]. Alternatively, when animals are actively moving along a track, prominent theta (6–12 Hz) oscillations appear in LFPs, and place cell sequences occur within individual theta cycles of ~120 ms (refs. 24–26). Such theta sequences have also been hypothesized as being involved in memory retrieval[27–29]. Although

previous studies have examined awake replay and theta sequences in various behavioral tasks, their proposed role in memory retrieval has not been established, mainly because the reward-based track-running tasks in these studies do not have a clear behavioral correlate with memory retrieval. The present study aimed to understand whether place cells encoding environments of aversive experience were reactivated during fear memory retrieval and whether the reactivation took place in the form of awake replay or theta sequences.

To this end, we recorded CA1 place cells while rats performed a linear inhibitory-avoidance (IA) task. In this task, rats first explored a 225-cm long track with two equally sized light and dark segments (**Fig. 1a**). After receiving mild footshocks in a shock zone (SZ), which was the end portion (1/8 of track length) of the dark segment, rats were placed back in the light segment and allowed to freely move around. The task is a linear version of the classical IA task, which is hippocampus-dependent and uses a box consisting of a light and a dark compartment[9,30,31]. Here we used a linear track instead of a box because the resulting sequential behavior allowed us to study place cell sequences. Since shocks occurred at the SZ, we expect animals to associate the aversive shocks with the SZ and thus avoid entering the SZ afterward. This avoidance behavior is a distinct behavioral correlate of memory retrieval, which would allow us to examine how place cells encoding a spatial context of fear memory (the SZ) are reactivated during memory retrieval. In addition, since rats would avoid the SZ after the shocks, any detected place cell activities associated with the SZ would occur due to memory retrieval, but not sensory cues at the SZ.

RESULTS

Animals display avoidance behavior in the linear IA task

We recorded from dorsal hippocampal CA1 neurons while four rats performed the linear IA task (**Fig. 1a**). On the first recording day (Day 1), animals explored the track in two 10–15 min sessions (Run 1 and Run 2), separated and followed by rests. On Day 2, they

---

[1]Neuroscience PhD Program, Baylor College of Medicine, Houston, Texas, USA. [2]Department of Molecular and Cellular Biology, Baylor College of Medicine, Houston, Texas, USA. [3]Department of Electrical and Computer Engineering, Rice University, Houston, Texas, USA. [4]Department of Neuroscience, Baylor College of Medicine, Houston, Texas, USA. Correspondence should be addressed to D.J. (dji@bcm.edu).
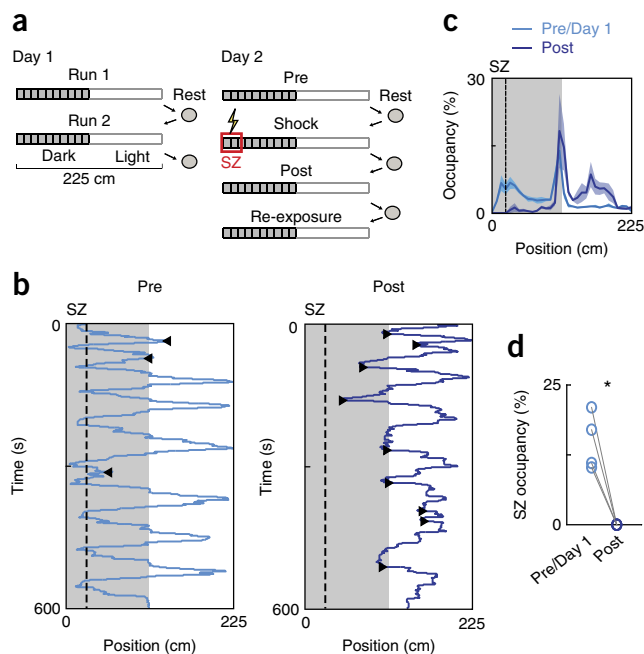
Figure 1 Behavior in the linear IA task. (**a**) Experimental procedure. On Day 1, rats were allowed to freely move on a two-segmented (light and dark) linear track in two sessions (Run 1, Run 2). On Day 2, rats freely moved in the same track before (Pre) and after (Post) receiving mild footshocks at a shock zone (SZ). Afterward, rats were placed in the SZ to make them travel through the entire track (re-exposure). The sessions were separated by resting in an enclosed box. The duration of every session and rest was 10–15 min. (**b**) A rat's trajectories in Pre and Post. Shaded area, positions in the dark segment; dashed line, boundary of SZ; arrowhead right (▶), SZ-avoiding turns; arrowhead left (◀), LE-avoiding turns. (**c**) Average percentage of time (mean ± s.e.m.) spent at each location (occupancy) of the track across all animals before (Pre/Day 1) and after (Post) the shocks. (**d**) Occupancy of each rat (circles) within the SZ in Pre/ Day 1 and Post. *$P = 0.01$, $t_3 = 5.8$, paired t-test ($n = 4$ rats).

first explored the track for 10–15 min (Pre). Following a rest, rats were placed in the light segment and two mild footshocks (1 s apart) were applied when they traveled to the SZ in the dark segment. Animals were then immediately removed from the track. After another rest, they were placed back in the light segment and allowed to explore freely for 10–15 min (Post). Finally, rats were manually placed in the SZ to make them travel through the entire track in another 10–15 min session (re-exposure). In Run 1, Run 2 and Pre, the animals traveled in both light and dark segments, with a preference for the dark segment (**Fig. 1b,c**; percentage of time spent in the dark: 74 ± 2%), reflecting their natural preference. In Post, the rats exhibited IA behavior: they tended to stay in the light segment (percentage of time in the light: 72 ± 8%) and completely avoided the SZ (**Fig. 1d**). In addition, the animals' speed was lower and they spent more time facing the SZ in Post than in Pre (**Supplementary Fig. 1**). During re-exposure, the animals occupied the SZ again, since they were manually placed there (**Supplementary Fig. 2**). To demonstrate the hippocampus-dependence of the linear IA task, we made lesions concentrated on the dorsal CA1 in a separate group of rats. We found that the SZ-avoidance behavior in Post was substantially reduced in the lesioned group, compared to that in a sham-lesioned group (**Supplementary Fig. 3**).

Awake replay leads to SZ cell reactivation during avoidance

We closely inspected the avoidance behavior in Post. We observed that, every time rats moved toward the SZ, they paused and then
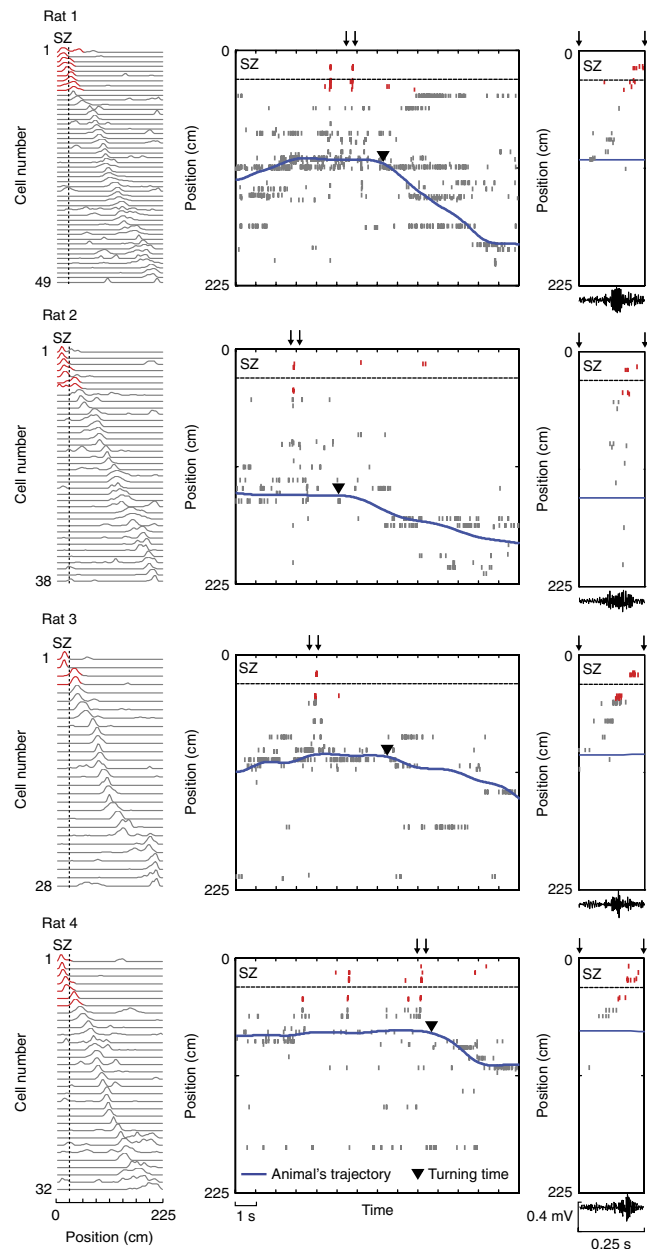

Figure 2 Sequential firing of place cells occurred before the first SZ-avoiding turn in every rat. Activities of track-active place cells are plotted for each of the four animals (Rat 1–Rat 4). Left: firing rate curves of place cells in Pre, each showing firing rate (normalized to its peak rate) of a cell along the track. Cells are ordered by peak locations. Red, place fields overlapping with the SZ; dashed line, SZ boundary. Middle: spike rasters of the same place cells as ordered on the left and the rat's trajectory during the first SZ-avoiding turn in Post. Each row shows spikes of a cell plotted at its peak firing location on the track (*y*-axis). Red, spikes of those cells with place fields overlapping with the SZ; dashed line, SZ boundary. Right: expanded view of the spike raster within a time window in the middle (arrows) and the filtered LFP in the ripple band within the same window (bottom). Note the sequential firing initiated by cells with place fields close to current locations and terminated by those with place fields in the SZ (red). Also note the simultaneous increase in ripple activity.

turned away before reaching the SZ. We refer to this action as an SZ-avoiding turn. Since turning away was the most obvious action for avoiding the SZ, memory retrieval likely occurred immediately
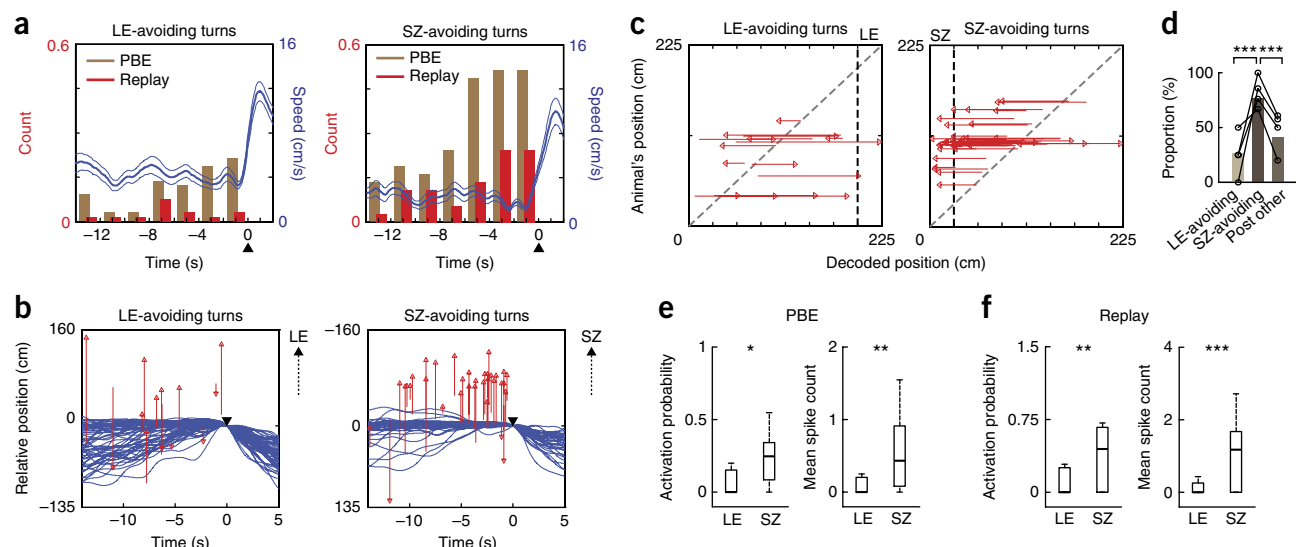
Figure 3 SZ-avoiding turns in Post were preceded by replay of place-cell activities leading to the SZ. (**a**) Counts of PBEs and replays within each 2-s bin of pausing, as well as animals' average speed (blue line, mean ± s.e.m.), around LE-avoiding turns in Pre/Day 1 and around SZ-avoiding turns in Post. The counts were normalized by number of turns. Up arrowheads (▲), turning time. (**b**) Replay trajectories during pausing (red), as well as animals' actual trajectories (blue), around LE-avoiding turns in Pre/Day 1 (n = 65 turns from all four rats) and around SZ-avoiding turns in Post (n = 37). The trajectories are aligned at the animal's position and time of turning (down arrowheads, ▼). Red arrowheads, end positions of replay trajectories; upward arrows, direction to the LE or SZ. (**c**) Same replay trajectories as in **b**, plotted against animals' positions (y-axis) on the track. Red arrowheads, end positions of replay trajectories; black dashed line, LE or SZ boundary; gray dashed line, equal animal and decoded positions. (**d**) Fraction of those replay trajectories during pausing that ended near the LE before LE-avoiding turns in Pre/Day 1 (LE-avoiding, n = 15), fraction of those that ended near the SZ before SZ-avoiding turns in Post (SZ-avoiding, n = 44) and fraction of those that ended near the SZ during the rest of the time periods in Post (Post other, n = 194). The fractions are plotted for each rat (circles) and for all animals combined (bar). ***P = 4×10^{-4} between LE-avoiding turns and SZ-avoiding turns and ***P = 1×10^{-5} between SZ-avoiding turns and Post other, binomial test; χ^2 test among all three types: P = 2×10^{-5}). (**e**) Activation probability and mean spike count of LE cells within PBEs during pauses before LE-avoiding turns in Pre/Day 1 and for the same measures of SZ cells within PBEs before SZ-avoiding turns in Post (n = 30 LE cells, 26 SZ cells; *P = 0.0057, **P = 0.0040, Wilcoxon rank-sum test. (**f**) As in **e**, but within replays. **P = 0.0039, ***P = 8×10^{-4}.

before these moments. Therefore, we first examined place-cell activity during pauses immediately before SZ-avoiding turns in Post on Day 2. Of a total of 329 CA1 neurons recorded from four rats on Day 1 and Day 2, 247 fired at specific locations of the track (place fields). Of these, 147 (28–49 per rat) had place fields on Day 2, as indicated by prominent peaks in their firing rate curves (firing rate at each position of the track; **Fig. 2**). We found that during pauses before SZ-avoiding turns in Post, those cells with place fields in the SZ were reactivated even though animals did not enter the SZ. As illustrated in **Figure 2**, this was observed during the first SZ-avoiding turn of every rat. Notably, the reactivation was accompanied by sequential firing of multiple place cells, during which cells with place fields close to the animals' current positions fired first and cells with place fields at the SZ fired last, and this sequential firing occurred together with increased ripple oscillations (**Fig. 2**). The observation suggests that the reactivation resulted from awake replay.

We quantified this observation for all SZ-avoiding turns in Post. To do so, we identified population burst events (PBEs) based on multiunit activities, which included all putative spikes recorded in the CA1. A PBE was defined as a time window (50–400 ms) with peak multiunit activity ≥4 s.d. above baseline. Because LFP ripple activity and population bursts of CA1 cells tend to occur concurrently[32,33], the PBEs identified as such were mostly those time periods associated with strong ripples (**Supplementary Fig. 4a,b**), as in previous studies[16,17,34]. We analyzed place cell sequences within PBEs. We constructed a template pattern from activities of 'template' cells, which displayed a single place field on the track in Pre (21–32 cells per rat). We defined those PBEs with at least four active template cells as

candidate events. For each candidate event, we determined whether it was a replay using a Bayesian approach: first decoding the spatial positions encoded by the firing pattern within the candidate event based on the template[35] and then statistically quantifying whether the decoded positions matched a trajectory on the track[17,18]. If they did, we categorized the PBE as a replay and the matched trajectory as its 'replay trajectory'. In constructing the templates, we did not separate place cell patterns on the animals' directions of movement[18], because the majority of place cells (70%) were bidirectional, i.e., they were active in both directions (toward or away from the SZ) with similar firing locations. Consequently, the majority of replays could not be distinguished as 'forward' or 'reverse' replays as in some previous studies[15,16] (**Supplementary Fig. 5**).

We identified PBEs and replays during pauses immediately before SZ-avoiding turns, referred to as SZ-avoiding PBEs and SZ-avoiding replays, respectively. There were 37 SZ-avoiding turns in Post in all four rats with an average of 9.3 ± 1.5 s spent pausing (no SZ-avoiding turns were detected in Pre or on Day 1; **Supplementary Fig. 6**). In Pre and on Day 1, since rats naturally tended to avoid light, they made turns before reaching the end zone of the light segment (LE). We refer to these turns as LE-avoiding turns. For comparison, we also analyzed pauses immediately before LE-avoiding turns and their associated LE-avoiding PBEs and replays. There were 65 LE-avoiding turns (**Supplementary Fig. 6**) in Pre and in Run 1 and Run 2 of Day 1 (Pre/Day 1), with an average of 4.7 ± 0.5 s spent pausing. As expected, during pauses before LE- and SZ-avoiding turns, PBEs and replays appeared (**Fig. 3a**), while the theta power of CA1 LFPs was low (**Supplementary Fig. 4c,d**). However, the rate of PBEs during pausing
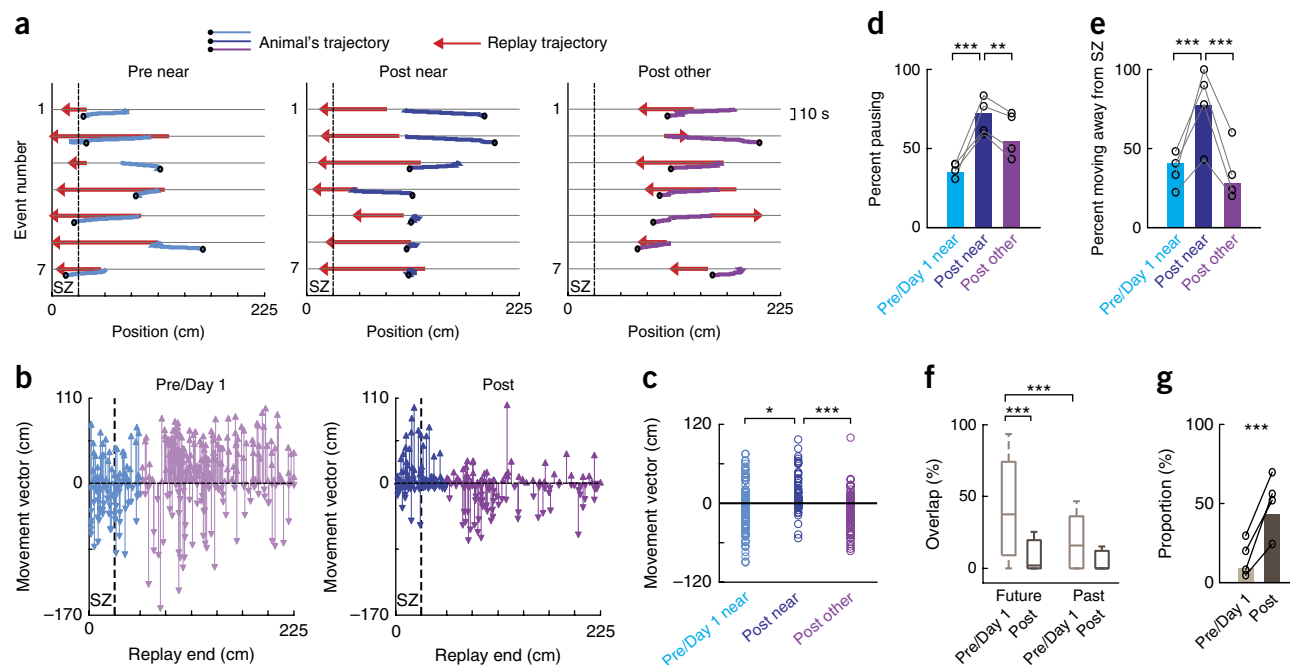
Figure 4 Replay trajectories ending near the SZ were followed by pausing and turning away from the SZ in Post. (**a**) Replay trajectories and the animal's moving trajectories within a 10-s window following replay, for the first seven replays that ended near the SZ in Pre (Pre near) and Post (Post near) and for the first 7 replay events that did not end near the SZ in Post (Post other) in an example rat. Dashed line, SZ boundary; black circle, animal's position at the end of the window. (**b**) Movement vectors following each replay, plotted at the end position of its replay trajectory (replay end), for all replays across all rats in Pre/Day 1 and in Post. The movement vectors following those replays ending near the SZ are plotted in blue (Post near) or light blue (Pre/Day 1 near). Other vectors are in purple (Post other) or light purple. Dashed line, SZ boundary. (**c**) Movement vectors following three types of replays: Pre/Day1 near, Post near and Post other (*$P = 0.0057$, $t_{218} = -2.8$; ***$P = 1 \times 10^{-6}$, $t_{236} = 5.0$, t-test; ANOVA comparing all three types: $P = 1 \times 10^{-4}$, $F_{2, 342} = 9.5$; $n = 107$ Pre/Day 1 near replays, 113 Post near replays and 125 Post other replays). (**d**) Proportion of movement vectors spent pausing among all vectors following the three types of replays, plotted for each rat (circles; $n = 4$) and for all animals combined (bars). ***$P = 2 \times 10^{-8}$ and **$P = 0.0037$, binomial test; χ^2 test comparing all three types: $P = 1 \times 10^{-7}$. (**e**) As in **d**, but for the proportion of movement vectors moving away from the SZ among nonpausing vectors (***$P = 8 \times 10^{-4}$ between Pre/Day 1 near and Post near; ***$P = 9 \times 10^{-6}$ between Post near and Post other, binomial test; χ^2 test among all three types: $P = 4 \times 10^{-5}$; $n = 70$ Pre/Day 1 near nonpausing vectors, 31 Post near nonpausing vectors and 57 Post other nonpausing vectors). (**f**) Overlaps between replay trajectories and animals' future or past trajectories for all replays in Pre/Day 1 and for those in Post (***$P = 1 \times 10^{-10}$ between future and past in Pre/Day 1, ***$P = 1 \times 10^{-26}$ between Pre/Day 1 and Post for future overlap, Wilcoxon rank-sum test; two-way ANOVA among all four overlaps: $P = 1 \times 10^{-13}$, future vs. past; $P = 6 \times 10^{-39}$, Pre/Day 1 vs. Post; $F_{1, 1, 1,163} = 56.3$ and 183.6, respectively; $n = 345$ Pre/Day 1 replays, 238 Post replays). (**g**) Proportions of replay trajectories that did not overlap with either animals' future or past trajectories out of those replay trajectories with nonpausing past or future movement in Pre/Day 1 and in Post, plotted for each rat (circles) and for all animals combined (bars). ***$P = 3 \times 10^{-19}$, binomial test; $n = 323$ Pre/Day 1 and 180 Post replays with nonpausing past or future movements.

was significantly greater before SZ-avoiding turns than before LE-avoiding turns (LE: 0.20 s⁻¹, SZ: 0.36 s⁻¹; $P = 1 \times 10^{-3}$, Wilcoxon rank-sum test; $n = 65$ LE-avoiding turns, 37 SZ-avoiding turns). The same was found for the rate of replays (LE: 0.05 s⁻¹, SZ: 0.13 s⁻¹, $P = 8 \times 10^{-5}$). The result indicates that PBEs and replays were more likely to occur before SZ-avoiding turns than before LE-avoiding turns.

We then closely examined replay trajectories of SZ-avoiding replays in Post and compared them with those of LE-avoiding replays in Pre/Day 1. Consistent with previous studies[17,18,36], replay trajectories tended to start from animals' current locations in both Post (correlation between animals' current locations and starting locations of replays: $r = 0.55$, $P = 2 \times 10^{-19}$, Pearson's r, $n = 238$) and in Pre/Day 1 ($r = 0.78$, $P = 1 \times 10^{-93}$, $n = 345$) and end further away, i.e., most replays were 'outward' (**Supplementary Fig. 5**). Notably, replay trajectories of SZ-avoiding replays were aligned toward the SZ (with their start-to-end locations pointing to the SZ), whereas those of LE-avoiding replays appeared much less aligned toward the LE (**Fig. 3b**). Plotting end locations of replay trajectories clearly showed that most replay trajectories of SZ-avoiding replays ended near the SZ (within 1/8 of the track length from the SZ boundary), but only a few LE-avoiding

replays ended near the LE (**Fig. 3c**). Indeed, the proportion of replay trajectories ending near the SZ among SZ-avoiding replays in Post was significantly greater than the proportion ending near the LE among LE-avoiding replays in Pre/Day 1 and significantly higher than the proportion among other replays in Post that occurred outside the pauses immediately before SZ-avoiding turns (**Fig. 3d**). Additional analysis suggested that this bias in replay trajectories toward the SZ in Post was not caused by the bias of animals' heading toward the SZ or the bias of animals' positions in the light segment per se (**Supplementary Fig. 7**). This finding indicates that, during pausing before SZ-avoiding turns, there was an increase in the replay of specific place-cell sequences encoding the paths from animals' current positions to the SZ.

The fact that most replay trajectories before SZ-avoiding turns ended near the SZ suggests that the cells with place fields at the SZ were reactivated before these turns in Post. To directly quantify this, we analyzed activation probability (probability of firing at least one spike in a PBE) and mean spike count of those cells with a single place field that overlapped with the SZ (SZ cells). We compared these measures of SZ cells within SZ-avoiding PBEs in Post to the same measures of cells with a single place field that overlapped with the
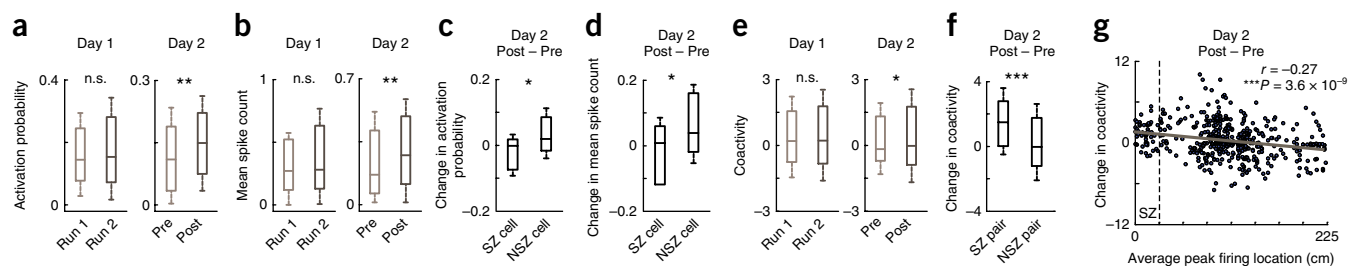
Figure 5 Shock experience altered place cell activity and coactivity within PBEs. (**a**) Activation probability of place cells within PBEs in Run 1 and Run 2 on Day 1 ($n = 100$) and that in Pre and Post on Day 2 ($n = 147$). Nonsignificant (n.s.): $P = 0.47$; **$P = 0.0018$, Wilcoxon signed-rank test. (**b**) As in **a**, but for mean spike count (n.s., $P = 0.70$; **$P = 0.0018$). (**c**) Change in activation probability from Pre to Post on Day 2 for SZ cells ($n = 26$) and NSZ cells ($n = 85$). *$P = 0.005$, Wilcoxon rank-sum test. (**d**) As in **c**, but for change in mean spike count (*$P = 0.027$). (**e**) Coactivity of pairs of place cells within PBEs in Run 1 and Run 2 on Day 1 ($n = 1,591$ pairs) and that in Pre and Post on Day 2 ($n = 2,424$). n.s., $P = 0.33$; *$P = 0.017$. (**f**) Changes in coactivity from Pre to Post on Day 2 for vicinity pairs with average peak locations near the SZ (SZ pairs, $n = 85$) and other vicinity pairs (NSZ pairs, $n = 385$). ***$P = 6 \times 10^{-7}$. (**g**) Change in coactivity within PBEs for every vicinity pair ($n = 470$) from Pre to Post on Day 2, plotted against their average peak firing location. Solid line, linear regression; r and P, correlation coefficient and associated P-value of the regression; dashed line, SZ boundary.

LE (LE cells) within LE-avoiding PBEs in Pre/Day 1. We found that both the activation probability and mean spike count of SZ cells were significantly greater than those of LE cells (**Fig. 3e**). Restricting the analysis to replays produced similar results (**Fig. 3f**). Furthermore, the activity of SZ cells, but not that of cells with place fields outside the SZ (non-SZ or NSZ cells), was substantially greater within SZ-avoiding PBEs than within other PBEs in Post (**Supplementary Fig. 8**). These results demonstrate that SZ cells were specifically reactivated during replays before SZ-avoiding turns in Post, even though animals did not physically enter the SZ.

Replay trajectories reflect paths to avoid
We have shown that replays before SZ-avoiding turns in Post largely ended their replay trajectories near the SZ. We next examined whether the converse was true, i.e., whether replay trajectories that ended near the SZ predicted the SZ-avoidance behavior. To this end, we identified all replays in Pre/Day 1 and in Post (**Supplementary Fig. 6**) and quantified animals' movement within a 10-s window following every replay by a 'movement vector', defined as a vector from the animal's position at the start to that at the end of the window (**Fig. 4a**). After aligning its start position to 0, a positive or negative movement vector would mean the animal moving away from or toward the SZ after the replay, respectively. **Figure 4b** shows movement vectors for all identified replays in Pre/Day 1 and Post. The absolute lengths of the vectors in Pre/Day 1 appeared greater than those in Post, apparently due to the fact that animals moved faster in Pre/Day 1 than in Post. We separated movement vectors for those replay trajectories ending near the SZ (Near) and those ending at other locations (Other) of the track. Movement vectors of Near replays in Post were significantly more positive than those of Near replays in Pre/Day 1 and more positive than those of Other replays in Post (**Fig. 4c**), indicating that Near replays in Post were followed by an increased tendency to avoid the SZ.

This tendency could be due to animals actively moving away from the SZ or pausing following a replay. To quantify this, we defined a small movement vector (between −10 and +10 cm) as an action of pausing, and an otherwise positive or negative vector as actively moving away or toward the SZ. We found that the proportion of pausing among Near replays in Post was indeed increased from that among Near replays in Pre/Day 1 and from that among Other replays in Post (**Fig. 4d**). Second, of the replays followed by a nonpausing movement, the proportion followed by moving away from the SZ was significantly greater for Near replays in Post than that for Near replays in Pre/Day 1 and that for Other replays in Post (**Fig. 4e**).

Thus, Near replays in Post were followed by animals either pausing or actively turning away from the SZ.

Our analyses suggest that many replay trajectories were those actively avoided by animals, which differs from previous findings that replay trajectories reflect animals' immediate past or future trajectory of actual movement, with a preference toward the future[15–17,21,36,37]. We directly measured how replay trajectories in our data reflected animals' immediate past or future moving trajectories. We defined an overlap between a replay trajectory and an animal's moving trajectory within a 10-s window before (past) or after (future) the replay as the proportion of the replay trajectory that was also included in the past or future trajectory. We found that the median overlap with future trajectories was significantly greater than that with past trajectories in Pre/Day 1, consistent with previous studies[36,37]. However, this overlap with future trajectories was greatly reduced in Post (**Fig. 4f**). More importantly, among those replays with nonpausing future or past trajectories, a large percentage of them (43%) did not overlap with either past or future trajectories at all in Post, and this percentage was significantly greater than that in Pre/Day 1 (**Fig. 4g**). These analyses directly confirm that trajectories actively avoided by animals were replayed in Post.

Shock experience alters place cell activities within PBEs
We next examined the impact of shock experience on place cell activities within PBEs. Both activation probability and mean spike count of track-active place cells within PBEs were significantly greater in Post than in Pre on Day 2 but not between Run 1 and Run 2 on Day 1 (**Fig. 5a,b**). However, the change in SZ cells was significantly less than that in NSZ cells (**Fig. 5c,d**). This difference between SZ and NSZ cells was largely because animals did not enter the SZ in Post, because place cell activities within PBEs were biased by animals' physical positions (**Supplementary Fig. 9a**). Indeed, when we restricted the analysis on those PBEs while animals were outside the SZ in Pre, this difference disappeared (**Supplementary Fig. 9b,c**). Despite the increase in place-cell activities within PBEs, there was no substantial change in percentage of replays among candidate events between Pre and Post (**Supplementary Fig. 10**). We then quantified whether the shock experience impacted coactivity, a measure of how pairs of place cells were activated together within PBEs[19,38]. We found a significant increase in the median coactivity of all place cell pairs from Pre to Post on Day 2 but not from Run 1 to Run 2 on Day 1 (**Fig. 5e**). In addition, we analyzed the coactivity specifically for those pairs of template cells with peak firing locations in the same vicinity (vicinity pairs,

defined as pairs with distances between peak locations of <35 cm). We found that vicinity pairs with their average peak location near the SZ (SZ pairs) increased coactivity significantly more than other vicinity pairs (NSZ pairs) in Post (**Fig. 5f**). Furthermore, plotting the coactivity change of every vicinity pair from Pre to Post revealed a significant correlation between the change and a pair's average peak location on the track (**Fig. 5g**), indicating that the closer a pair's peak locations were to the SZ, the stronger the increase in their coactivity. Restricting the analysis to PBEs occurring outside the SZ produced similar results (**Supplementary Fig. 9d,e**). These results indicate that the shock experience intensified place-cell activity within PBEs in general and specifically enhanced the coactivity of place cells with peak locations near the SZ.

SZ cells are barely reactivated in theta sequences

Our results suggest that SZ cells were reactivated via awake replay during fear memory retrieval in Post. We next examined the hypothesis that SZ cells could also be activated in theta sequences in Post. We identified 3,471 theta cycles in Post and found that overall place cell activity within theta cycles was relatively low, compared to that within PBEs in Post (mean spike count expressed as median, 25% and 75% values, theta: 0.03, 0.006 and 0.12, respectively; PBE: 0.26, 0.10 and 0.46, respectively; $P = 7 \times 10^{-23}$, $n = 147$ cells, Wilcoxon signed-rank test). To analyze place cell sequences within theta cycles, we identified 516 theta cycles in Post with at least three active template cells as candidate cycles[29,39]. Using the same Bayesian decoding method as in identifying replays, we determined whether the decoded positions within a candidate cycle matched a trajectory of the track. If so, we referred to the firing sequence within the candidate as a theta sequence (**Fig. 6a**) and the matched trajectory as a theta trajectory. We identified 133 theta sequences (26% of candidate cycles) and their theta trajectories in Post from four rats (**Supplementary Fig. 11**). Unlike many replay trajectories, which extended to and ended near the SZ, theta trajectories were relatively local and rarely reached the SZ in Post (**Fig. 6b**). The median length of theta trajectories was significantly shorter than that of replay trajectories (**Fig. 6c**). Only 4.5% of theta trajectories either ended or started near the SZ, and this percentage was much lower than the percentage of replay trajectories (49%) that ended or started near the SZ (**Fig. 6d**), indicating very little activation of SZ cells in theta sequences in Post. Indeed, this near absence of SZ cell activity resulted in significantly lower activation probability and mean spike count of SZ cells in theta sequences than in replays (**Fig. 6e**). Furthermore, not only was the activity of SZ cells low within theta sequences, it was generally low in all periods outside identified PBEs, compared with that of NSZ cells (firing rate outside PBEs, expressed as median, 25% and 75% values, SZ cells: 0.025, 0.0098 and 0.076 Hz, respectively, $n = 26$; NSZ cells: 0.40, 0.19 and 0.95 Hz, respectively, $n = 85$; $P = 7 \times 10^{-9}$, Wilcoxon rank-sum test). These results clearly show that SZ cells were barely activated in theta sequences in Post, suggesting that theta sequences were not directly involved in the retrieval of fear memory at the SZ.

Shock experience induces partial remapping

Previous studies show that some place cells change their firing locations (i.e., remap) after fear conditioning[40–43]. We therefore examined whether and how place cells remapped following the shock experience in our experiment. For this purpose, we analyzed changes in place cell activities on the track between Pre and re-exposure and compared them to those between Run 1 and Run 2 on Day 1 (**Fig. 7a** and **Supplementary Fig. 12**). We first examined the changes at the population level. For each position on the track in a session, we
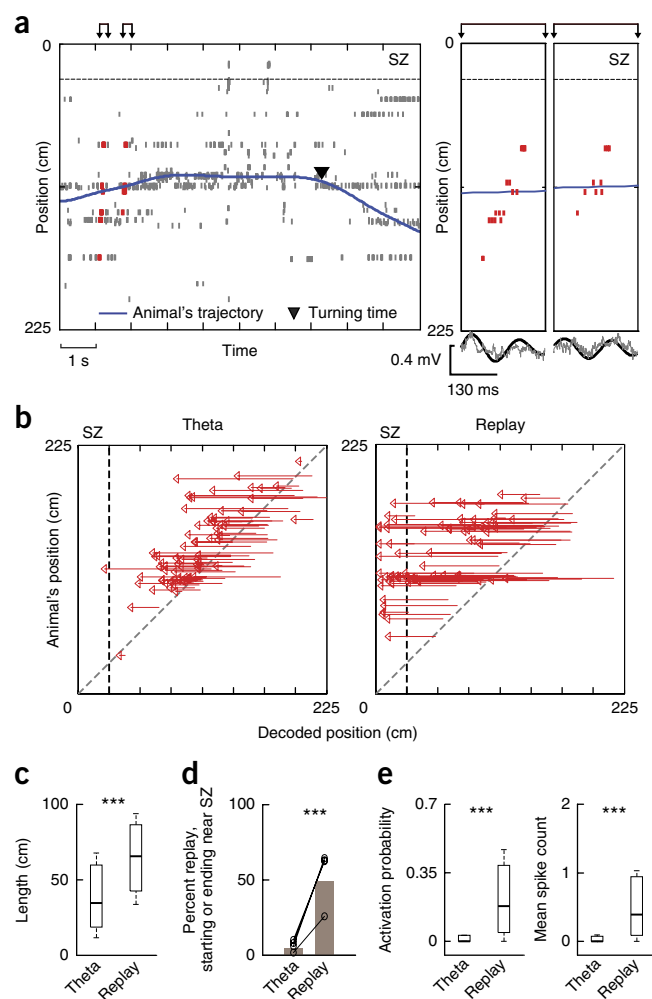

Figure 6 Theta sequences did not reactivate SZ cells in Post. (**a**) The plot is arranged similarly to the middle and right panels in **Figure 2**, but here shows theta sequences. Left: spike rasters of place cells before an SZ-avoiding turn in Post. Spikes in identified theta sequences are shown in red. Right: expanded view of two example theta sequences from left (arrows) and associated raw (gray) and filtered LFP trace within the theta band (black). (**b**) Theta trajectories and replay trajectories in Post, plotted against animals' positions on the track. All identified theta trajectories pointing toward the SZ from all four animals are plotted ($n = 77$). For replay trajectories, we plotted a random sample of 77 of 191 SZ-pointing replay trajectories. Dashed line, SZ boundary. (**c**) Trajectory lengths of theta ($n = 133$) and replay ($n = 238$) trajectories in Post (***$P = 4 \times 10^{-11}$, Wilcoxon rank-sum test). (**d**) Percentages of theta and replay trajectories that ended or started near the SZ, among all theta and replay trajectories in Post, plotted for each rat (circles; $n = 4$) and for all animals combined (bars). ***$P = 4 \times 10^{-15}$, binomial test. (**e**) Activation probability and mean spike count of SZ cells ($n = 26$) within theta sequences and replays in Post (***$P = 8 \times 10^{-6}$ for both activation probability and mean spike count, Wilcoxon signed-rank test).

defined a population vector (PV), which consisted of firing rates of all active cells at that position. We then computed a PV correlation between Pre and re-exposure on Day 2 or between Run 1 and Run 2 on Day 1 for each position. The median PV correlation of all track positions on Day 2 was modestly (26%) but significantly reduced from that on Day 1 (**Fig. 7b**), indicating that remapping had occurred between Pre and re-exposure. However, the Day 2 correlations remained high (median, 25% and 75% correlations: 0.58, 0.36 and 0.74, respectively)
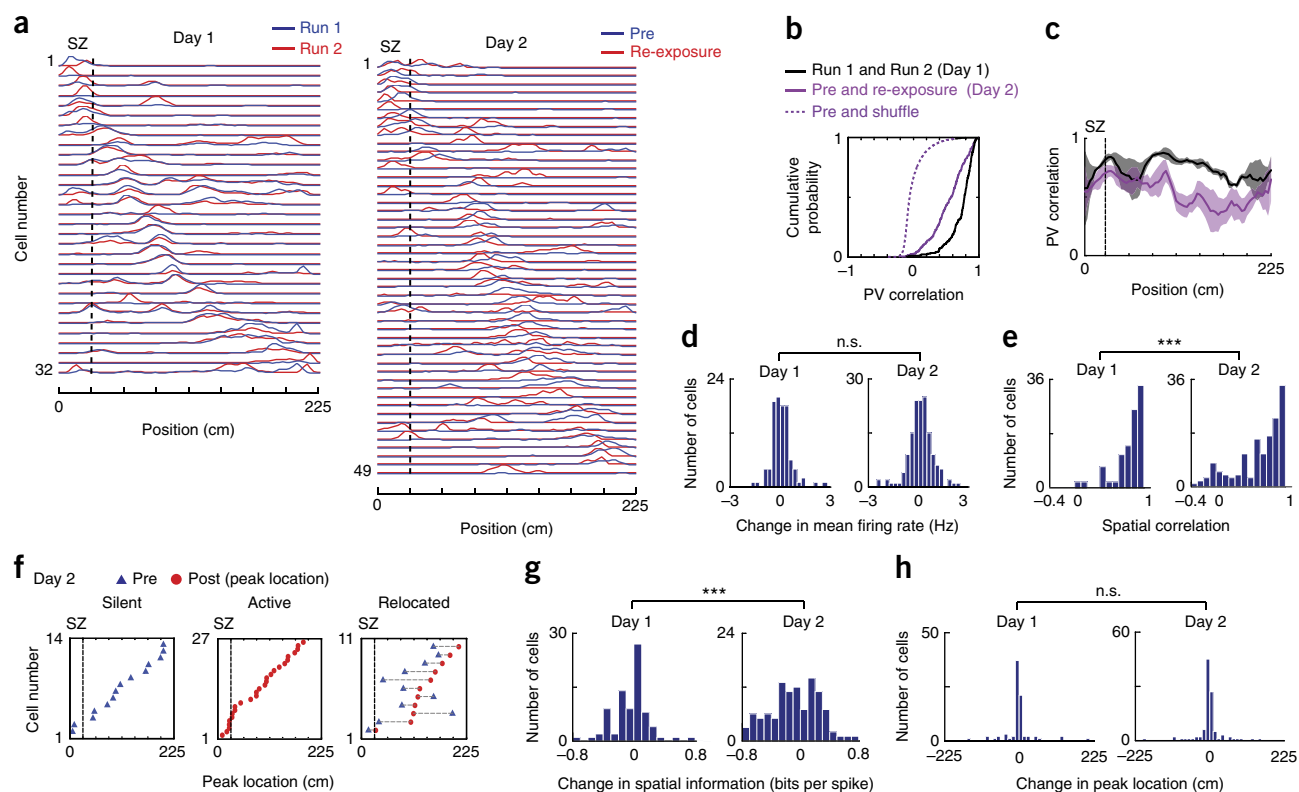
Figure 7 Shock experience triggered partial remapping of place cells. (**a**) Firing rate curves of place cells in Run 1 and Run 2 on Day 1, and Pre and re-exposure on Day 2 for an example rat. Firing rates are normalized to the maximum rate between two sessions on the same day. Cells are ordered by peak firing locations in Run 1 or Pre along the track (x-axis). (**b**) Cumulative distributions of PV correlations between Run 1 and Run 2, between Pre and re-exposure, and between Pre and shuffled Pre ($P = 6 \times 10^{-18}$, between Run 1 and Run 2 vs. between Pre and re-exposure; $P = 1 \times 10^{-133}$, between Pre and re-exposure vs. between Pre and shuffled Pre (shuffle); Wilcoxon rank-sum test; $n = 216$ PV correlations between Run 1 and Run 2, 288 PV correlations between Pre and re-exposure and 288,000 PV correlations between Pre and shuffle. (**c**) PV correlations (mean ± s.e.m.) along the track between Run 1 and Run 2 on Day 1, and between Pre and re-exposure on Day 2. Note that PV correlations within the SZ were relatively similar between Day 1 and Day 2 ($P = 0.08$, Wilcoxon rank-sum test). (**d**) Distributions of mean firing rate change between Run 1 and Run 2 on Day 1 ($n = 100$ cells) and between Pre and re-exposure on Day 2 ($n = 147$). n.s., $P = 0.07$, Levene's test for variance comparison; t-test for mean comparison: $P = 0.33$, $t_{245} = 0.97$. (**e**) As in **d**, but for distributions of spatial correlation (***$P = 2 \times 10^{-5}$, Wilcoxon rank-sum test). (**f**) Peak firing locations in Pre and re-exposure of those place cells that became silent, became active or relocated from Pre to re-exposure on Day 2. Each row is a cell. Dashed line, SZ boundary. (**g,h**) Distributions of (**g**) spatial information change and (**h**) peak location shift between Run 1 and Run 2 on Day 1 and between Pre and re-exposure on Day 2 for those cells active in both sessions ($n = 80$ on Day 1, 106 on Day 2; ***$P = 1 \times 10^{-4}$ in **g**; n.s. ($P = 0.83$) in **h**, Levene's test for comparing variances; Wilcoxon rank-sum test for comparing medians: $P = 0.73$ in **g**, $P = 0.97$ in **h**).

and were much greater than that computed with shuffled data[44], suggesting that the remapping from Pre to re-exposure was partial[42]. Despite this partial remapping, the median PV correlations for positions within the SZ were not significantly different between Day 2 and Day 1 (**Fig. 7c**), suggesting that the SZ was not a special target for remapping. In addition, to understand when the remapping occurred, we restricted the analysis of PV correlations to only those positions visited by animals in Post and found that much of the remapping occurred in Post with additional remapping occurring in re-exposure (**Supplementary Fig. 13**).

Next, we quantified place-cell activity changes between sessions at the level of individual cells by several measures. First, we computed the change in mean firing rate. The rate change between Pre and re-exposure on Day 2 was similar to that between Run 1 and Run 2 on Day 1, except that it appeared more broadly distributed on Day 2, but comparing variances showed that the difference did not reach significance (**Fig. 7d**). Second, we computed a spatial correlation for each cell, as the Pearson correlation between its rate curves in two sessions. We found that the median spatial correlation between Pre and re-exposure for cells on Day 2 was slightly (15%) but significantly

reduced from that between Run 1 and Run 2 on Day 1 (**Fig. 7e**), suggesting, again, partial remapping after the shocks. Overall, 81% of the cells (119 of 147) had significant spatial correlation ($P \leq 0.01$, Pearson's r) on Day 2, compared to 96% (96 of 100) on Day 1 ($P = 5 \times 10^{-4}$, binomial test). Third, we computed the proportion of cells (among all place cells) that were silent or active in the first session but became active or silent, respectively, in the second session. We found that 18% (27 of 147) became active and 9.5% (14 of 147) became silent from Pre to re-exposure on Day 2, but these proportions were not statistically different from those between Run 1 and Run 2 on Day 1 (12% (12 of 100) became active, $P = 0.18$; 8.0% (8 of 100) became silent; $P = 0.68$, binomial test). In addition, we considered a cell active in both sessions without significant spatial correlation ($P > 0.01$, Pearson's r) as a relocated cell. We found only a small percentage (10%, 11 of 106) of relocated cells between Pre and re-exposure on Day 2, which was greater than the percentage (2.5% or 2 of 80, $P = 0.037$, binomial test) between Run 1 and Run 2 on Day 1. Cells that became either active or silent and cells that relocated on Day 2 had peak locations were distributed all over the track, without any bias toward the SZ (**Fig. 7f**), confirming that the SZ was not a

special target for remapping. Finally, for each cell active in both sessions on a given day, we computed a change in spatial information[45] and a shift in peak firing location (peak shift) between the two sessions. The median of spatial information change on Day 2 was not significantly different from that on Day 1, but the distribution showed a significantly greater variance (i.e., it was more broadly distributed; **Fig. 7g**), consistent with the idea that the fear experience on Day 2 induced partial remapping without a systematic increase or decrease in spatial tuning of place cells. The distributions of peak shift on both days show a dominant peak around 0 and were not significantly different (**Fig. 7h**). In fact, a large percentage had only a small shift in their firing locations (absolute shift < 14 cm, half the width of the SZ) on either Day 2 (74%) or Day 1 (74%). Taken together, these results indicate that, although the shock experience induced partial remapping, the majority of place cells did not alter their firing locations after the shocks.

Given this finding, we reanalyzed our data to examine how the replay and theta trajectories in Post would change if we used the templates generated from place cell activities in re-exposure instead of those in Pre. We found that the number of replays detected in Post and the results on replay trajectories remained similar (**Supplementary Fig. 14**). Using templates in re-exposure also produced similar results on theta sequences (**Supplementary Fig. 15**). This reanalysis thus suggests that the partial remapping did not dramatically alter place cell firing patterns in replays and theta sequences in Post.

DISCUSSION

To understand how place cells are activated in fear memory retrieval, we analyzed CA1 place cells before and after rats received footshocks in the SZ of a linear track. We have shown that, during pauses before SZ-avoiding turns in Post, place cell patterns representing the trajectories from animals' current locations to the SZ were replayed within PBEs, which led to the reactivation of SZ cells. Such timed correlation between avoidance behavior and awake replay did not occur before the shock experience. Conversely, replays that ended near the SZ were followed by animals pausing or moving away from the SZ, but this occurred only following the aversive experience. In contrast to replays, SZ cells were not reactivated within theta cycles in Post, and theta trajectories did not reach the SZ. Since the SZ-avoidance behavior was apparently due to retrieval of the fear memory associating the SZ with footshocks, our data strongly suggest that awake replay, but not theta sequence, supported fear memory retrieval in IA behavior.

How awake replay participates in memory processing has been under scrutiny. One hypothesis is that awake replay is involved in memory retrieval[23]. Recent studies find that replay trajectories are biased toward animals' actual future trajectories[22,36,37], and disrupting awake replay impairs future choices in a spatial working memory task[46]. These findings lead to the idea that awake replay is for planning[36]. Since memory retrieval is a crucial, if not necessary, component of planning, this idea does not necessarily contradict the memory retrieval hypothesis. However, these findings could also mean that replay trajectories reflect the outcome of planning (future trajectory), rather than recall of stored trajectories in memory. These possibilities are hard to distinguish in previous studies, because there are no clear behavioral correlates of memory retrieval in the reward-based tasks that these studies employed. Our study shows that, immediately before SZ-avoiding turns in Post, place cell sequences representing the paths from animals' current positions to the SZ were replayed. As a result, these replay trajectories did not correlate with animals' actual immediate future or past trajectories but with the trajectories

that animals actively avoided. This strongly suggests that awake replay primarily reflected not the outcome of planning but recall of stored trajectories. Second, replay trajectories extended all the way to the SZ and SZ cells were reactivated in Post, even though the animals did not enter the SZ. This result means that the replayed place cell sequences were not driven by current sensory experience in Post but, notably, resulted from relatively remote spatial experience that occurred previously. Our findings thus provide strong evidence for the hypothesis that awake replay is a substrate of memory retrieval.

An important question is then how fear memory was retrieved during the linear IA task. In this task, rats first learned to associate shocks with the SZ, which was likely encoded by SZ cells. The shocks (learning) presumably induced an association between SZ cells and shock-related neurons in the basolateral amygdala, similarly to the process that occurs in contextual fear conditioning[10,47]. We found that SZ cells were reactivated before SZ-avoiding turns in Post, apparently due to the retrieved aversive shock experience. This finding suggests a retrieval scheme in which SZ cells were reactivated first, followed by the reactivation of those shock-related amygdalar neurons, which then reactivated the aversive experience and triggered the avoidance behavior. In this scheme, hippocampal place cells encoded spatial contexts in which aversive or appetitive events occurred. Retrieval of these events could be triggered or initiated by the retrieval of their spatial contexts. This scheme is consistent with recent results showing that optogenetic manipulation of hippocampal cells active in particular spatial contexts can lead to altered place-avoidance or place-preference behavior[13,48,49].

Our data show that SZ cells were reactivated via awake replay of place cell sequences encoding the paths from animals' current positions to the SZ, which revealed a precise place cell pattern of how spatial contexts were reactivated in IA behavior. This finding suggests that place cells at animals' current locations activated neighboring place cells in a chain reaction that ultimately reactivated the SZ cells. This chain reaction was likely initiated by sensory cues at current locations and followed by the activation of synaptic connections that resided in the hippocampal CA3 area, where extensive recurrent networks exist and ripple oscillations originate[33]. Notably, we found that SZ cells were more likely to fire together during PBEs after the shocks than other cells, which could possibly result from a scenario in which synapses among those CA3 cells that innervate the CA1 SZ cells are preferentially potentiated by the shock experience at the SZ. This experience-dependent potentiation may have effected the preferential replay of the trajectory from animals' current position to the SZ, which eventually reactivated the exact context (the SZ) where aversive experiences took place and triggered fear memory retrieval. This could be a general model for how place cells participate in the retrieval of episodic memories.

In this model, hippocampal place cells represent spatial contexts where aversive events take place. A question is whether this representation is modified by the aversive events. In our experiment, the shock experience induced partial remapping of place cell activities between Pre and re-exposure. Quantitatively, only 19% of place cells were found to have uncorrelated firing rate curves between Pre and re-exposure, and only 26% of cells active in both sessions shifted their peak firing locations more than half the width of the SZ. In addition, using templates in Pre and re-exposure produced similar results in our replay and theta sequence analyses. These data suggest a largely stable spatial representation, with a modest degree of modification after the shock experience. This finding is different from previous studies that show more robust remapping after fear conditioning[40,42]. However, there are important differences between our task and those

in the previous studies. In one study[40], rats were food-restricted and constantly foraged for food rewards in a conditioning box before and after being shocked 16 times (periorbital shocks). In another study[42], rats were exposed to a predator odor for 5 min. Thus, reward was present in one study and the aversive stimuli in both studies (multiple shocks, prolonged exposure to predator) were much stronger than that used in our experiment (two milder shocks). It is likely that different appetitive and/or aversive experiences can cause different amounts of remapping.

Hypothesized substrates of memory retrieval include ripple-associated awake replay as well as theta sequences[27,29]. Within single theta cycles of CA1 LFPs, place cells with neighboring place fields fire one after another in a sequence similar to the actual behavioral sequence[24–26,39]. Previous studies found that such sequences can reflect future spatial trajectories and activate remote reward locations[28,50]. However, in our experiment, we observed very little activation of SZ cells in theta sequences in Post. Theta trajectories appeared short and did not extend to the SZ, suggesting that theta sequences were relatively local and seemed insufficient to reactivate the spatial context of fear memory in our task. However, we need to point out that the speed of animals in our task was generally low compared to that in a typical reward-based track-running task. Since there is evidence that the length of theta trajectory is proportional to speed[39], the low speed might explain the short and local nature of theta trajectories in Post. For this reason, theta sequences may not be optimal for reactivating remote spatial locations when animals' speed is low. Therefore, our data provide evidence that ripple-associated awake replay, rather than theta sequences, is a substrate for retrieving spatial contexts of fear memory at least in IA and similar tasks.

METHODS

Methods, including statements of data availability and any associated accession codes and references, are available in the online version of the paper.

Note: Any Supplementary Information and Source Data files are available in the online version of the paper.

1. Scoville, W.B. & Milner, B. Loss of recent memory after bilateral hippocampal lesions. *J. Neurol. Neurosurg. Psychiatry* **20**, 11–21 (1957).
2. Corkin, S. What's new with the amnesic patient H.M.? *Nat. Rev. Neurosci.* **3**, 153–160 (2002).
3. Tulving, E. & Donaldson, W. *Organization of Memory* (Academic Press, 1972).
4. O'Keefe, J. & Nadel, L. *The Hippocampus as a Cognitive Map* (Oxford University Press, 1978).
5. Leutgeb, S. *et al.* Independent codes for spatial and episodic memory in hippocampal neuronal ensembles. *Science* **309**, 619–623 (2005).
6. Miller, J.F. *et al.* Neural activity in human hippocampal formation reveals the spatial context of retrieved memories. *Science* **342**, 1111–1114 (2013).
7. O'Keefe, J. & Dostrovsky, J. The hippocampus as a spatial map. Preliminary evidence from unit activity in the freely-moving rat. *Brain Res.* **34**, 171–175 (1971).
8. Wilson, M.A. & McNaughton, B.L. Dynamics of the hippocampal ensemble code for space. *Science* **261**, 1055–1058 (1993).
9. Izquierdo, I., Furini, C.R. & Myskiw, J.C. Fear Memory. *Physiol. Rev.* **96**, 695–750 (2016).
10. Maren, S., Phan, K.L. & Liberzon, I. The contextual brain: implications for fear conditioning, extinction and psychopathology. *Nat. Rev. Neurosci.* **14**, 417–428 (2013).
11. Phillips, R.G. & LeDoux, J.E. Differential contribution of amygdala and hippocampus to cued and contextual fear conditioning. *Behav. Neurosci.* **106**, 274–285 (1992).
12. Liu, X. *et al.* Optogenetic stimulation of a hippocampal engram activates fear memory recall. *Nature* **484**, 381–385 (2012).
13. Ramirez, S. *et al.* Creating a false memory in the hippocampus. *Science* **341**, 387–391 (2013).
14. Garner, A.R. *et al.* Generation of a synthetic memory trace. *Science* **335**, 1513–1516 (2012).
15. Foster, D.J. & Wilson, M.A. Reverse replay of behavioural sequences in hippocampal place cells during the awake state. *Nature* **440**, 680–683 (2006).
16. Diba, K. & Buzsáki, G. Forward and reverse hippocampal place-cell sequences during ripples. *Nat. Neurosci.* **10**, 1241–1242 (2007).
17. Davidson, T.J., Kloosterman, F. & Wilson, M.A. Hippocampal replay of extended experience. *Neuron* **63**, 497–507 (2009).
18. Karlsson, M.P. & Frank, L.M. Awake replay of remote experiences in the hippocampus. *Nat. Neurosci.* **12**, 913–918 (2009).
19. Singer, A.C. & Frank, L.M. Rewarded outcomes enhance reactivation of experience in the hippocampus. *Neuron* **64**, 910–921 (2009).
20. Carr, M.F., Karlsson, M.P. & Frank, L.M. Transient slow gamma synchrony underlies hippocampal memory replay. *Neuron* **75**, 700–713 (2012).
21. Jackson, J.C., Johnson, A. & Redish, A.D. Hippocampal sharp waves and reactivation during awake states depend on repeated sequential experience. *J. Neurosci.* **26**, 12415–12426 (2006).
22. Gupta, A.S., van der Meer, M.A., Touretzky, D.S. & Redish, A.D. Hippocampal replay is not a simple function of experience. *Neuron* **65**, 695–705 (2010).
23. Carr, M.F., Jadhav, S.P. & Frank, L.M. Hippocampal replay in the awake state: a potential substrate for memory consolidation and retrieval. *Nat. Neurosci.* **14**, 147–153 (2011).
24. Skaggs, W.E., McNaughton, B.L., Wilson, M.A. & Barnes, C.A. Theta phase precession in hippocampal neuronal populations and the compression of temporal sequences. *Hippocampus* **6**, 149–172 (1996).
25. Dragoi, G. & Buzsáki, G. Temporal encoding of place sequences by hippocampal cell assemblies. *Neuron* **50**, 145–157 (2006).
26. Foster, D.J. & Wilson, M.A. Hippocampal theta sequences. *Hippocampus* **17**, 1093–1099 (2007).
27. Lisman, J. & Redish, A.D. Prediction, sequences and the hippocampus. *Phil. Trans. R. Soc. Lond. B* **364**, 1193–1201 (2009).
28. Johnson, A. & Redish, A.D. Neural ensembles in CA3 transiently encode paths forward of the animal at a decision point. *J. Neurosci.* **27**, 12176–12189 (2007).
29. Zheng, C., Bieri, K.W., Hsiao, Y.T. & Colgin, L.L. Spatial sequence coding differs during slow and fast gamma rhythms in the hippocampus. *Neuron* **89**, 398–408 (2016).
30. Stubley-Weatherly, L., Harding, J.W. & Wright, J.W. Effects of discrete kainic acid-induced hippocampal lesions on spatial and contextual learning and memory in rats. *Brain Res.* **716**, 29–38 (1996).
31. McGaugh, J.L. The amygdala modulates the consolidation of memories of emotionally arousing experiences. *Annu. Rev. Neurosci.* **27**, 1–28 (2004).
32. Buzsáki, G., Horváth, Z., Urioste, R., Hetke, J. & Wise, K. High-frequency network oscillation in the hippocampus. *Science* **256**, 1025–1027 (1992).
33. Csicsvari, J., Hirase, H., Mamiya, A. & Buzsáki, G. Ensemble patterns of hippocampal CA3-CA1 neurons during sharp wave-associated population events. *Neuron* **28**, 585–594 (2000).
34. Ji, D. & Wilson, M.A. Coordinated memory replay in the visual cortex and hippocampus during sleep. *Nat. Neurosci.* **10**, 100–107 (2007).
35. Zhang, K., Ginzburg, I., McNaughton, B.L. & Sejnowski, T.J. Interpreting neuronal population activity by reconstruction: unified framework with application to hippocampal place cells. *J. Neurophysiol.* **79**, 1017–1044 (1998).
36. Pfeiffer, B.E. & Foster, D.J. Hippocampal place-cell sequences depict future paths to remembered goals. *Nature* **497**, 74–79 (2013).
37. Singer, A.C., Carr, M.F., Karlsson, M.P. & Frank, L.M. Hippocampal SWR activity predicts correct decisions during the initial learning of an alternation task. *Neuron* **77**, 1163–1173 (2013).
38. Cheng, S. & Frank, L.M. New experiences enhance coordinated neural activity in the hippocampus. *Neuron* **57**, 303–313 (2008).
39. Gupta, A.S., van der Meer, M.A., Touretzky, D.S. & Redish, A.D. Segmentation of spatial experience by hippocampal θ sequences. *Nat. Neurosci.* **15**, 1032–1039 (2012).
40. Moita, M.A., Rosis, S., Zhou, Y., LeDoux, J.E. & Blair, H.T. Putting fear in its place: remapping of hippocampal place cells during fear conditioning. *J. Neurosci.* **24**, 7015–7023 (2004).
41. Wang, M.E., Yuan, R.K., Keinath, A.T., Ramos Álvarez, M.M. & Muzzio, I.A. Extinction of learned fear induces hippocampal place cell remapping. *J. Neurosci.* **35**, 9122–9136 (2015).

42. Wang, M.E. *et al.* Long-term stabilization of place cell remapping produced by a fearful experience. *J. Neurosci.* **32**, 15802–15814 (2012).

43. Kelemen, E. & Fenton, A.A. Key features of human episodic recollection in the cross-episode retrieval of rat hippocampus representations of space. *PLoS Biol.* **11**, e1001607 (2013).

44. Miao, C. *et al.* Hippocampal remapping after partial inactivation of the medial entorhinal cortex. *Neuron* **88**, 590–603 (2015).

45. Skaggs, W.E., McNaughton, B.L., Gothard, K.M. & Markus, E.J. An information-theoretic approach to deciphering the hippocampal code. in *Advances in Neural Information Processing Systems* (eds. Hanson, S.J., Cowan, J.D. & Giles, C.J.) 1030–1037 (Morgan Kaufmann, 1993).

46. Jadhav, S.P., Kemere, C., German, P.W. & Frank, L.M. Awake hippocampal sharp-wave ripples support spatial memory. *Science* **336**, 1454–1458 (2012).

47. Zelikowsky, M., Hersman, S., Chawla, M.K., Barnes, C.A. & Fanselow, M.S. Neuronal ensembles in amygdala, hippocampus, and prefrontal cortex track differential components of contextual fear. *J. Neurosci.* **34**, 8462–8466 (2014).

48. Redondo, R.L. *et al.* Bidirectional switch of the valence associated with a hippocampal contextual memory engram. *Nature* **513**, 426–430 (2014).

49. Trouche, S. *et al.* Recoding a cocaine-place memory engram to a neutral engram in the hippocampus. *Nat. Neurosci.* **19**, 564–567 (2016).

50. Wikenheiser, A.M. & Redish, A.D. Hippocampal theta sequences reflect current goals. *Nat. Neurosci.* **18**, 289–294 (2015).

ONLINE METHODS

Animals, behavioral task and experimental procedure. Four adult (400–500 g) male Long-Evans rats (Rat 1–Rat 4) were used in recording experiments. Animals were individually housed with standard 12-h:12-h light/dark cycles and normal diets. Experiments were performed during the light cycle. Each rat was surgically implanted, under isoflurane (1–2.5%) anesthesia, with a microdrive containing 24 tetrodes targeting the bilateral CA1 of dorsal hippocampus (12 tetrodes in each hemisphere; 3.8 mm posterior and 2.4 mm lateral to bregma). Tetrodes were made by twisting together four nichrome wires (diameter 13 μm; Sandvik Palm Coast, Palm Coast, FL), each electroplated with gold to an impedance of 200–300 kΩ. After surgery, tetrodes were lowered to the CA1 pyramidal layer over 2–3 weeks. All experimental procedures were approved by the Institutional Animal Care and Use Committee at Baylor College of Medicine and followed National Institute of Health guidelines.

Tetrode recordings were conducted while rats performed an IA task on a linear track. The track was 225 cm long and 8 cm wide with 18-cm high walls, and contained a dark and a light segment of equal length. The light and dark segments had a white plastic and a metal grid floor, respectively. A dim light was placed above the light segment. The last 28 cm (1/8 of the track length) of the metal grid floor in the dark segment (shock zone, SZ) was connected to a shock apparatus (Harvard Apparatus, Holliston, MA). The wire bundle connecting the tetrode microdrive to recording equipment was anchored to the ceiling at a point aligned with the center of the track. No food reward was given on the track. Before recording started, all animals were introduced to the track and explored for 10 min for at least 1 d. On the first recording day (Day 1), CA1 cells of Rat 1–Rat 3 were recorded while they explored the track for two sessions (Run 1 and Run 2), separated and followed by rest sessions in a rest box. This Day 1 recording was omitted for Rat 4. On Day 2, CA1 cells of Rat 1–Rat 4 were recorded while they went through a series of track and rest sessions (**Fig. 1a**). First, rats explored the track for a session (Pre), followed by a rest session. Rats were then placed in the light segment of the track, and two mild foot shocks (each 0.4 mA, 1 s duration with 1-s intershock intervals) were applied as soon as they entered the SZ. The recording was paused during this brief shock session (< 4 min) to avoid recording the noise generated by the shocks. Immediately after the shocks, rats were removed from the track and placed in the rest box for another rest session. Afterward, they were placed back in the light segment for another track session (Post), with their heads initially facing the end of the light segment. Following one more rest, animals were brought to the track for a re-exposure session, during which they were manually placed in the SZ if they stayed outside of the SZ for more than 2–3 min. For Rat 1 and Rat 4, all recording and rest sessions were 10 min. For Rat 2 and Rat 3, all sessions were 15 min. Although Rat 4 was recorded without the Day 1 procedure, the data on Day 2 from all four rats were included in the analysis. We repeated the analysis excluding the Rat 4 data and results remained very similar (data not shown).

Animals were euthanized after recording by pentobarbital overdose (200 mg/kg). A current (30 μA) was passed to each tetrode for ~15 s to create a small lesion at its tip. Brains were fixed in 10% formalin for at least 24 h, sectioned at 50–100 μm thickness and stained with 0.5% cresyl violet. Tetrode recording locations were verified from lesions in the stained sections. Only cells recorded from the CA1 pyramidal layer were used in further analyses.

Data acquisition. All data were collected using a Digital Lynx system (Neuralynx, Bozeman, MT). LFPs were digitally filtered between 0.1 Hz to 1 kHz and recorded at 2,034 Hz. Action potentials (spikes) were identified by a threshold of 60 μV and recorded at 32 kHz. The positions and head directions of animals were tracked by two LEDs (green and red) mounted over the animal's head and an overhead video-tracking system. Position data were sampled at 33 Hz.

Behavioral analysis. We defined an SZ-avoiding turn as an action that started with facing the SZ, followed by a 180° whole body turn. To identify such a turn, we smoothed an animal's head direction at each timepoint with a moving average filter (0.5-s window). We detected epochs when head direction first crossed 180° (facing the SZ) and then crossed 15° or 345° for clockwise or counterclockwise turning, respectively. We then visually inspected the videos during these epochs to verify the whole-body turning. Turning time was defined as the first time angular velocity first exceeded 30° s^{-1}. To detect pauses before turning, animals' speed was similarly smoothed with a 0.5-s window. For each turn, we defined

the pausing period as the time window before a turn when the speed was lower than 3 cm/s. To identify LE-avoiding turns, we also designated the last 28 cm of the light segment (same width as the SZ) as the light end (LE). The LE boundary was thus 28 cm from the end of the light segment. We identified LE-avoiding turns and their pauses in Pre and on Day 1, similarly to the way we identified SZ-avoiding turns.

Place cell quantification. Spikes were sorted into single units (spikes presumably fired by individual neurons) by manual clustering using xclust (M.A. Wilson, MIT; https://github.com/wilsonlab/mwsoft64/tree/master/src/xclust). We quantified spatial firing properties of individual neurons. Putative interneurons (mean firing rate > 15 Hz) were excluded from the analysis. The firing rate curve of a neuron in a session was its firing rate at each 3.1-cm bin along the track, which was the total spike count within the bin divided by the total amount of time the animal spent in the bin, and smoothed by a Gaussian kernel with a 6.2-cm s.d. (standard deviation). Spikes occurring within population burst events (PBEs; see below) and when rats were stationary (speed < 3 cm/s) were excluded from the spike count. The firing rate curve was computed from spiking activities on any movement direction. We did not compute a separate firing rate curve for each movement direction in our main results because we found that most cells (63% on Day 1 and 76% on Day 2; see also **Supplementary Fig. 5**) were bidirectional (peak firing rates on each of the two moving directions > 1.5 Hz and with correlated firing rate curves between the two directions). For each day, a neuron was considered as an active place cell on the track if its maximum rate exceeded 1.5 Hz in at least one track session. Further analysis was performed only on these track-active cells. For each cell, we determined the peaks of its firing rate curve, each identified as the maximum among a group of consecutive spatial bins with rates >1.5 Hz. A cell was considered to have multiple place fields if its rate curve had at least two peaks that were separated by at least 35 cm; otherwise it was a cell with a single place field. We found that the majority of cells (92% on Day 1 and 93% on Day 2) with either single or multiple place fields in one session continued to have single or multiple place fields in another session on the same day.

We defined a place cell as an SZ cell if it had a single place field and had a maximum firing rate within the SZ greater than 20% of the peak of its firing rate curve in either Pre or re-exposure. A cell was defined as a non-SZ cell (NSZ cell) if it had a single place field and its maximum firing rate within the SZ was less than 20% of the peak of its firing rate curve in both Pre and re-exposure. Similarly, we defined a place cell as an LE cell if it had a single place field with its maximum rate within the LE greater than 20% of its peak rate on the track in Pre on Day 2 or in Run 1/Run 2 on Day 1.

Place cell remapping. We quantified remapping between two sessions of a given day by PV correlation, spatial correlation and changes in mean firing rate, spatial information and firing location. To compute PV correlation between two sessions, we constructed a population vector (PV), consisting of firing rates of all active cells, at each spatial bin of the track in each session. A PV correlation was the Pearson correlation between the two PVs at each bin. For PV correlations involving Post (**Supplementary Fig. 13**), the bins in and close to the SZ were excluded from this analysis, since animals did not travel to the SZ in Post. To assess the distribution of PV correlation at the chance level, we shuffled Pre PVs by randomly assigning cell identities and circularly shifting the cells' rate curves on the track 1,000 times, and then we computed PV correlations between the actual and shuffled PVs[44]. For each place cell, spatial correlation was the Pearson correlation of its rate curves between two sessions[5]. A cell was determined to become silent or active from one session to another if it was active first (peak rate > 1.5 Hz) and then became inactive (peak rate ≤ 1.5 Hz) or vice versa. For cells active in both sessions, we defined a cell as relocated if its spatial correlation was not significant (*P* > 0.01). For these cells, we also computed changes in their peak firing location and firing precision, which was quantified by spatial information[45].

Population burst events (PBEs) and LFP analysis. PBEs were defined from multiunit activity, which included all putative spikes recorded by all tetrodes in the CA1 on a given day[16,17,34]. Multiunit spikes were counted in each 10-ms time bin. A PBE was defined as a time period of 50–400 ms within which the peak spike count exceeded the mean by at least 4 s.d. The start and end of the PBE were timepoints when the spike count crossed the mean.

To verify that PBEs were associated with strong ripple oscillations in the CA1 LFPs[16,17,34], for each recoding day we performed two analyses on the LFP trace

of a tetrode channel histologically identified as at the CA1 pyramidal layer. First, we analyzed how the ripple oscillation increased its amplitude within PBEs. The LFP trace was bandpass filtered within the ripple band (100–250 Hz) and then Hilbert transformed. The absolute values (amplitudes) of the Hilbert transform were smoothed using a Gaussian kernel with a 4-ms s.d. Amplitudes were then normalized by their mean and s.d. as z-scores. Second, we computed power spectrograms of raw LFPs triggered by PBEs by a multitaper method (http://chronux.org/) using 100-ms time windows. We obtained the s.d. and mean for each frequency across all windows and normalized the power of that frequency at each window as a z-score[36]. The PBE-triggered spectrogram was triggered at the peak of multiunit activity. We then computed the z-scored power of 100-ms sliding windows with a 10-ms step size at the interval (−350, +350) ms around the multiunit peak.

For analyzing theta power before LE/SZ-avoiding turns, we filtered LFPs within the theta band (6–12 Hz). Theta amplitudes (obtained by Hilbert transform of the filtered LFPs) were z-scored relative to the mean and s.d. of amplitudes in a session and then smoothed by a Gaussian kernel with a 1-s s.d.

Place cell activity and coactivity within PBEs. For each cell active in a session, we computed activation probability (probability of firing at least one spike) and mean spike count (average number of spikes) within a PBE. For a pair of active place cells, we quantified how they coactivated together in PBEs by a measure of coactivity[19,38]. Briefly, for a pair of cells A and B, if they were independently active in n_A and n_B events out of N PBEs, the number of events expected from chance during which both were active had a mean, $E = n_A n_B / N$, and a variance, $\sigma^2 = n_A n_B (N-n_A)(N-n_B)/N^2(N-1)$. The coactivity was the actual number of events during which both cell were active (n_{AB}) normalized by the expected mean and s.d., $z = (n_{AB}-E)/\sigma$. We computed coactivity for all pairs of active cells and specifically for those pairs of template cells (see below) that had peak firing locations in the same vicinity (vicinity pairs, i.e., pairs with peak firing locations < 35 cm apart). The change in coactivity for a vicinity pair from Pre to Post on Day 2 was linearly regressed with the average of their peak firing locations.

Identification of theta cycles. We identified individual theta cycles of LFPs in track sessions. For each rat, we selected the electrode with highest time-averaged theta power and with at least one place cell for analysis. We filtered LFPs within theta (6–12 Hz), delta (1–4 Hz) and ripple (100–250 Hz) bands. We then determined envelopes of both theta and delta by Hilbert transform, and computed the ratio of theta to delta envelopes at each timepoint. High-theta time windows were identified as those in which the theta/delta ratio exceeded 2 (refs. 28,29) and when peak ripple power (absolute amplitude) was less than 3 s.d. above the mean. Within these high-theta time windows, we identified peaks of the theta-filtered LFP (theta peaks). For each theta peak, we determined the local minimum of neuronal spiking activity that was nearest to the peak. The spiking activity was computed by counting spikes from all neurons in 1-ms time bins and smoothed with a 10-ms Gaussian kernel. The consecutive nearest local minima of theta peaks were used as start/end times of individual theta cycles for the theta sequence analysis below[29,39].

Identification of replays and theta sequences. We identified replays and theta sequences by a Bayesian decoding method[17,18,35]. First, we constructed a firing template by taking firing rate curves of all place cells with single place fields (template cells) in either Pre or re-exposure. We used cells with single place fields because including place cells with multiple place fields could generate spurious decoded locations, since these cells could be contaminated by other cells that could not be differentiated by tetrodes. Nevertheless, we also performed the replay analysis using the templates made of all active place cells, including those with multiple place fields, and the results were similar (data not shown). In addition, since most place cells (70%) were bidirectional (**Supplementary Fig. 5**), the templates were not built from place cell activities separately on each of animals' two moving directions on the track but from rate curves averaged over both directions[18]. Each firing rate curve of a cell in a template was used to compute a prior firing probability of the cell at each location of the track, assuming a Poisson firing process.

To identify replays, we defined a PBE with at least four active template cells as a candidate event. For each 20-ms time bin (with a step of 10 ms) within a candidate event that had at least one spike, we computed a spatial probability distribution by Bayes' rule according to the prior firing probability[35]. The 'decoded' position at each time bin was the location of the track with the maximum posterior

probability. We then performed a linear regression between decoded positions and time bin numbers[18]. The resulting R^2 value, a measure of how well the decoded positions matched to a linear trajectory on the track, was compared to 1,000 shuffle-generated R^2 values. For each of these shuffled values, we randomly shuffled the decoded positions in time and recomputed the R^2 value of the linear regression. The P-value was the proportion of shuffles with R^2 values greater than the actual R^2 value. A candidate event was considered a replay if $P < 0.05$. Its replay trajectory was determined by its linear regression, which was a spatial vector from the regressed position at the first decoded time bin with at least one spike to that at the last decoded time bin with at least one spike, capped within the range of the track (i.e., between 0 and 225 cm).

To identify theta sequences, we selected those theta cycles with at least three template cells firing at least one spike as candidate cycles[28,39]. We decoded the positions within 20-ms time bins (with a step of 10 ms) within each candidate cycle. We then determined whether the decoded positions significantly matched a trajectory on the track, similarly to the way we identified replays. If so, we defined the place cell sequence within the candidate cycle as a theta sequence and the matched trajectory as a theta trajectory.

Replay trajectory, movement vector and overlap with past and future trajectories. A replay trajectory was considered ending near the SZ (Near replay) if its end position was within the SZ or less than 28 cm from the SZ boundary (within the last quarter of the track in the dark segment). Otherwise, it was considered an 'other' replay. Similarly, a replay trajectory was considered ending near the LE if its end position was within the LE or less than 28 cm from the LE boundary (within the last quarter of the track in the light segment).

For each replay, we analyzed the animal's movement following the replay by a movement vector. We defined a (future) time window of 10 s immediately after the end time of the replay. The movement vector was a spatial vector from the animal's position at the start to the end of the window. An animal's movement was defined as moving toward the SZ, moving away from the SZ, or pausing if the movement vector was <−10 cm, >+10 cm or between −10 and +10 cm, respectively. We computed the overlap between a replay trajectory and the animal's immediate past or future moving trajectory. We defined a future time window of 10 s as above in computing movement vectors and defined a past time window as the 10-s period immediately preceding the start of a replay. The overlap between a replay trajectory and a past (or future) trajectory was the percentage of locations along the replay trajectory that were covered by the animal's past (or future) trajectory. For computing the percentage of replays that had no overlap with either future or past trajectory, we used only those replays with at least 10 cm of movement within their future and past time windows.

Forward, reverse, outward and inward replays. We detected replays using templates built from average place cell activities on the track (overall templates). To understand these replays in more details (**Supplementary Fig. 5**), we also characterized these replays using templates (unidirectional templates) built from place cell activities when animals moving through the track on each of the two moving directions. The vast majority of replays (89%) identified by overall templates significantly replayed at least one unidirectional template. (Conversely, 83% of replays identified by unidirectional templates significantly replayed the overall template.) If a PBE replayed only one unidirectional template but not the other, it was further defined as a forward or a reverse replay if its replay trajectory pointed toward (start-to-end locations) the same or opposite direction of the replayed unidirectional template, respectively[15,16]. For those PBEs that replayed both unidirectional templates (bitemplate replays), the overlap between two replay trajectories decoded from two unidirectional templates was the ratio of the length of their overlapped portion to their average length. Finally, we defined a replay as outward if the start position of its replay trajectory was closer to the animal's current position than the end position or inward if vice versa.

Hippocampal lesion and behavioral testing. To examine whether the linear IA task depends on the hippocampus, an additional 18 adult (350–400 g), male Long-Evan rats were used in the lesion experiment. Each rat was randomly assigned to a control ($n = 9$) or a lesion group ($n = 9$). Neurotoxic lesions in the dorsal CA1 of the lesion group were created during surgery, by infusing NMDA (Sigma-Aldrich, St. Louis, MO) at 20 μg/μL in a vehicle of 100-mM phosphate-buffered saline (PBS, pH = 7.4). NMDA was infused to three sites bilaterally, using a microinfusion pump (KD Scientific; Holliston, MA) and a 10-μL Hamilton

syringe (Hamilton; Reno, NV) at a rate of 0.1 μL/min. The coordinates of the three infusion sites targeting the dorsal CA1 of each hemisphere were: 3.6 mm posterior to the bregma (AP), 1.0 mm lateral to the midline (ML) and 2.4 mm ventral to the dura (DV); AP: 3.6 mm, ML: 2.0mm and DL: 2.1 mm; and AP: 3.6 mm, ML: 3.0 mm and DV: 2.3 mm. The infusion volume was 0.1 μL for the first two sites and 0.15 μL for the third. Later histological analysis verified that lesions occurred predominantly in the dorsal CA1 and that the ventral hippocampus was intact (**Supplementary Fig. 3**). For the control group, vehicle alone without NMDA was similarly injected at the same coordinates.

At least 7 d after the surgery, each rat was tested in the linear IA task. On Day 1, rats freely explored on the track for 20 min. On Day 2, rats first freely explored the track for 10 min (Pre) and were then returned to their home cages briefly (<1 min). In the following shock session, rats were placed in the light segment of the track. Two mild footshocks (each 0.4 mA, 1 s duration, 1-s intershock interval) were applied as soon as they traveled to the SZ. Immediately after the shocks, rats rested in their home cages for 10 min. Animals were placed back in the light segment and allowed to freely explore for 10 min (Post). During all sessions, an LED light was mounted on the rats' bodies to track their positions. Animals in this lesion experiment on average spent less time around the center of the track than the animals in the recording experiment, because their heads were not connected to a wire bindle that was balanced at the center. After behavioral testing, animals were killed for histological analysis, as in the recording experiment. The experimenter was blind to the group allocation during behavioral testing and data analysis of this experiment.

Statistical analysis. No formal methods were used to predetermine sample sizes; the sample sizes used here are similar to those used in the field[15–18]. For statistical analysis, we used Student's *t*-tests and ANOVA for normally distributed data (after testing for data normality), and we used Wilcoxon rank-sum tests or Wilcoxon signed-rank tests for non-normally distributed data. All tests were two-sided. For multiple comparisons, we used Bonferroni's corrections to adjust the significance levels. We did not exclude any data points. In box plots, horizontal lines are the median and the 25% and 75% range values; whiskers present the most extreme data points ≤ 1 (**Fig. 3e,f**) or ≤0.5 (box plots in other figures) interquartile range from box edges. A **Supplementary Methods Checklist** is available.

Data and code availability. The data and code that support the findings of this study are available from the corresponding author upon reasonable request.